Neuron, Vol. 25, 29–41, January, 2000, Copyright ©2000 by Cell Press

Neuropilin-2 Is Required In Vivo for Selective Axon Guidance Responses to Secreted Semaphorins

Roman J. Giger,* Jean-François Cloutier,*‖ Amar Sahay,*‖ Rabinder K. Prinjha,†‖ Dorothy V. Levengood,* Stephen E. Moore,† Susan Pickering,‡ David Simmons,† Sohaila Rastan,‡ Frank S. Walsh,† Alex L. Kolodkin,*§ David D. Ginty,*§ and Martin Geppert‡

*Department of Neuroscience
The Johns Hopkins University School of Medicine
Baltimore, Maryland 21205
†Department of Neuroscience
‡Department of Comparative Genetics
SmithKline Beecham
Third Avenue
Harlow, Essex, CM19 5AW
United Kingdom

Summary

Neuropilins are receptors for class 3 secreted semaphorins, most of which can function as potent repulsive axon guidance cues. We have generated mice with a targeted deletion in the *neuropilin-2* (*Npn-2*) locus. Many *Npn-2* mutant mice are viable into adulthood, allowing us to assess the role of Npn-2 in axon guidance events throughout neural development. Npn-2 is required for the organization and fasciculation of several cranial nerves and spinal nerves. In addition, several major fiber tracts in the brains of adult mutant mice are either severely disorganized or missing. Our results show that Npn-2 is a selective receptor for class 3 semaphorins in vivo and that Npn-1 and Npn-2 are required for development of an overlapping but distinct set of CNS and PNS projections.

Introduction

Nervous system function critically depends on the proper wiring of neural circuits. During development, growth cones of extending axons navigate their way, often over long distances, into their target fields, where they form synapses with appropriate postsynaptic partners. It is becoming clear that pathfinding by most axons is dependent upon a complex combination of secreted and membrane-bound growth cone attractants and repellents (Mueller, 1999). Recently, several families of growth cone guidance molecules have been identified. These include the netrins, ephrins, slits, and semaphorins. Moreover, receptors for members of each of these families of guidance cues have been identified, although their modes of intracellular signaling remain unclear. The identification of growth cone guidance cues and their receptors, in combination with the ability to selectively disrupt genes encoding these proteins, provides an important opportunity to understand the specific roles played by these proteins during development of the mammalian nervous system.

The semaphorin family is a large phylogenetically conserved family of genes whose members encode secreted, transmembrane, and GPI-anchored proteins, many of which have been shown to function as axon guidance cues during neural development (Mark et al., 1997). All semaphorins have a signature sema domain approximately 500 amino acids in length. Based upon the presence of structural motifs C-terminal to the sema domain and their mode of membrane attachment, semaphorins have been subdivided into seven classes (Goodman et al., 1999). The six known class 3 semaphorins, which include mammalian Sema3A, Sema3C, and Sema3F, are secreted proteins that function as potent chemorepellents for specific classes of CNS and PNS neurons in vitro. Sema3A is essential for neural development since mice lacking this secreted semaphorin exhibit severe defects in projections of cranial and spinal nerves (Taniguchi et al., 1997). Class 3 semaphorins are expressed in unique and dynamic patterns during development of the vertebrate CNS and PNS.

Recently, cell surface receptors for semaphorins have been identified. The neuropilins, a small family of type I transmembrane proteins that includes neuropilin-1 (Npn-1) and neuropilin-2 (Npn-2), bind class 3 semaphorins with high affinity (Chen et al., 1997; He and Tessier-Lavigne, 1997; Kolodkin et al., 1997). Npn-1 binds with high affinity to Sema3A, Sema3C, and to Sema3F (Chen et al., 1997; Feiner et al., 1997). Npn-1 function is necessary for Sema3A-mediated repulsive guidance events both in vitro and in vivo, and genetic ablation of *Npn-1* phenocopies neuronal defects observed in *Sema3A* mutant mice (Kitsukawa et al., 1997). Together, these results indicate that Npn-1 is a Sema3A receptor and is required for normal neural development. In addition, severe defects in the cardiovascular system are observed in *Npn-1* mutant mice, probably due to a requirement for semaphorin signaling for cardiovascular development and/or a requirement for Npn-1 as a receptor for select isoforms of vascular endothelial growth factor ($VEGF_{165}$) (Kitsukawa et al., 1995, 1997; Soker et al., 1998; Kawasaki et al., 1999). Npn-2 also functions as a receptor for class 3 semaphorins. Npn-2 binds with high affinity to Sema3C and Sema3F, but it binds poorly, if at all, to Sema3A (Chen et al., 1997). Npn-2 is necessary for Sema3F- but not Sema3A-mediated repulsion of sympathetic neurons in vitro, and both Npn-1 and Npn-2 are thought to be required for Sema3C function in vitro (Chen et al., 1998; Giger et al., 1998; Takahashi et al., 1998). Npn-1 and Npn-2 are expressed in overlapping but largely distinct populations of developing neurons (Kawakami et al., 1996; Chen et al., 1997; Kolodkin et al., 1997). Thus, specificity of signaling for each of the class 3 semaphorins is established, at least in part, by their ability to bind to either Npn-1 and/or Npn-2.

A second large family of proteins, the plexins, contains

§To whom correspondence should be addressed (e-mail: dginty@jhmi.edu [D. D. G.], kolodkin@jhmi.edu [A. L. K.]).
‖These authors contributed equally to this work.

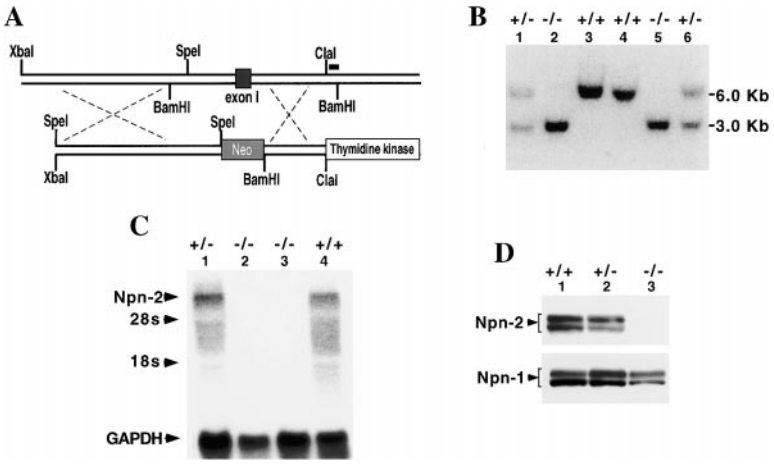

Figure 1. Generation and Molecular Characterization of *neuropilin-2* Mutant Mice

(A) Structure of part of the *Npn-2* gene including exon 1, which encodes the amino terminal 24 amino acids of Npn-2. Below is a summary of the *Npn-2* gene targeting vector. Homologous recombination should generate a mutant allele that lacks exon 1 and an additional 1.7 kb of upstream DNA. The position of the outside probe used for genotyping by Southern blot is indicated.

(B) Southern blot analysis of six P1 pups derived from *Npn-2* heterozygous intercrosses. Genomic DNA was digested with BamHI and subjected to Southern blot analysis. The blot was probed with a radiolabeled 246 bp Npn-2 probe, indicated in 1A. Sizes of the expected wild-type and mutant alleles are 6.0 and 3.0 kb, respectively.

(C) Northern blot analysis of RNA isolated from four E15 embryos derived from *Npn-2* heterozygous intercrosses. Genotype analysis was performed on the same embryos, and the indicated genotypes of the mice are listed above the lanes. *Npn-2* mRNA was not observed in RNA samples extracted from *Npn-2* homozygous mutant mice even after long exposures of the blots. Blots were stripped and rehybridized with a probe to GAPDH.

(D) Npn-1 and Npn-2 immunoblot analysis of protein extracts prepared from brains of three P1 pups derived from *Npn-2* heterozygous intercrosses. Antibodies generated against the Npn-1 or Npn-2 C domain were previously described and do not cross-react (Giger et al., 1998). Genotype analysis was performed on the same pups, and the indicated genotypes of the mice used for immunoblot analysis are listed above the lanes.

several members that have recently been shown to be semaphorin receptors both in invertebrates and in vertebrates (Comeau et al., 1998; Winberg et al., 1998; Takahashi et al., 1999; Tamagnone et al., 1999). While vertebrate class 3 secreted semaphorins bind directly to neuropilins, they do not bind directly to plexins (Takahashi et al., 1999; Tamagnone et al., 1999). However, members of other classes of semaphorins do bind directly to plexins (Tamagnone et al., 1999). Plexins and neuropilins show patterns of coexpression in the vertebrate nervous system, neuropilins and plexins can form complexes in vitro, and functional data obtained in vitro from both neuronal and nonneuronal cells demonstrate that plexin A1 is necessary for Sema3A repulsion and growth cone collapse (Ohta et al., 1992, 1995; Satoda et al., 1995; Takahashi et al., 1999; Tamagnone et al., 1999). Together, these data support the idea that neuropilins are ligand binding subunits and plexins are signaling subunits of class 3 semaphorin holoreceptor complexes.

To gain insight into the role played by Npn-2 in signaling specific axon guidance events mediated by class 3 semaphorins in vivo, we generated mice with a targeted deletion in the *Npn-2* locus. In contrast to *Npn-1* mutant mice, which die during the second half of gestation (Kitsukawa et al., 1997), many *Npn-2* mutant mice are viable into adulthood. This allowed us to assess the role played by Npn-2 throughout neural development. We find that Npn-2 is required for organization and fasciculation of several cranial nerves and spinal nerves. Furthermore, we show that several major fiber tracts in the brains of adult mutant mice are either severely disorganized or entirely missing. Our results show that Npn-2 is a receptor for a subset of class 3 semaphorins in vivo and that Npn-1 and Npn-2 are required for development of an overlapping, but largely distinct, set of CNS and PNS projections.

Results

Generation of *Neuropilin-2* Mutant Mice

Homologous recombination in embryonic stem cells was performed using a targeting vector designed to replace exon 1 and an additional 1.7 kb of upstream sequences of *Npn-2* with a neomycin expression cassette (Figure 1A). Exon 1 encodes the first 24 amino acids of Npn-2 including the entire signal sequence, loss of which should impair targeting of truncated Npn-2 protein to the plasma membrane. In addition, deletion of presumptive promoter sequences upstream of exon 1 is likely to reduce or eliminate expression of *Npn-2*. Two targeted ES cell lines were identified, and one that was injected into blastocysts gave rise to a germline-transmitting male chimera. One mouse harboring the mutant allele, I-225, was used to generate a line that was backcrossed into a C57BL/6 genetic background. Heterozygous *Npn-2* mutant mice were mated, and neonates homozygous for the mutant allele were obtained (Figure 1B). Genotype analysis revealed approximate Mendelian frequencies for embryos obtained at embryonic day 11 (E11), E15, and E18, which indicates that *Npn-2*$^{-/-}$ mice are viable at these times of gestation (Table 1; data not shown). *Npn-2*$^{-/-}$ mice are born, and their external appearance is indistinguishable from wild-type and heterozygous littermates. However, neonatal and adult mutant mice are obtained at reduced Mendelian frequencies (Table 1). Moreover, we observed an increased rate of mortality of neonatal and juvenile

Table 1. Viability of *Npn-2* Mutant Mice

Genotype	+/+	+/−	−/−	Total
E10-E18	65 (27%)	109 (45%)	68 (28%)	242
P1-P5	31 (26%)	69 (58%)	18 (15%)	107
P5-adult	64 (48%)	48 (36%)	22 (16%)	134

Npn-2$^{-/-}$ mice compared to their wild-type and *Npn-2*$^{+/-}$ littermates, although many mutants did survive to adulthood. The number of juvenile and adult *Npn-2*$^{-/-}$ mice obtained from intercrosses of *Npn-2*$^{+/-}$ mice that were backcrossed four or more generations to a C57BL/6 genetic background was very low (data not shown). Adult *Npn-2*$^{-/-}$ females are fertile, but they produce litters with very few offspring. Homozygous mutant males are very poor breeders, and most of them are sterile.

We next assessed expression of *Npn-2* in mutant and control littermates. Northern blot analysis using RNA extracted from E15 embryos revealed a single transcript of ~6 kb in wild-type and heterozygous mice, but no transcript was detected in *Npn-2*$^{-/-}$ embryos (Figure 1C). Western blotting was done using extracts prepared from brains of P1 animals and two previously characterized antibodies that selectively recognize the c domains of either Npn-1 or Npn-2 (Kolodkin et al., 1997; Giger et al., 1998). While Npn-1 protein was found in brain extracts prepared from wild-type, heterozygous, and homozygous mutant mice, Npn-2 protein was found in brains of wild-type and heterozygous mice but not in brains from *Npn-2*$^{-/-}$ mice (Figure 1D). Thus, *Npn-2*$^{-/-}$ mice have undetectable levels of Npn-2 mRNA and protein, and, therefore, can be considered *Npn-2* null mutants. The penetrance of all phenotypes described below was 100%.

Selective Loss of Endogenous Binding Sites for Sema3F and Sema3C but Not Sema 3A in Brains of *Npn-2*$^{-/-}$ Mice

Previous work indicated that Npn-2 is a receptor for the secreted semaphorin, Sema3F (Chen et al., 1997; Giger et al., 1998). Thus, we used the *Npn-2*$^{-/-}$ mice to determine whether Npn-2 is the major binding site for Sema3F and/or other class 3 semaphorins in brain. To visualize endogenous binding sites for Sema3F in neonatal brain tissue, we incubated sections of P1 mouse forebrain with an alkaline phosphatase-tagged Sema3F ligand (APSema3F). Then, APSema3F binding sites were identified using an in situ alkaline phosphatase reaction (Cheng and Flanagan, 1994). Robust binding of APSema3F was observed within the hippocampus and in afferent and efferent hippocampal projections, including the fimbria and fornix, in sections from wild-type mouse brain (Figure 2A). Moreover, strong APSema3F binding was found in the medial habenula and the fasciculus retroflexus (habenulo-interpeduncular tract). This APSema3F binding pattern is consistent with the previous observations that *Npn-2* is strongly expressed in the septum, the dentate gyrus, the CA3, and to a lesser extent the CA1 fields within the hippocampus, and in the medial habenula (Chen et al., 1997; Chédotal et al., 1998; Giger et al., 1998). In contrast to robust binding of APSema3F to brain sections of wild-type mice, little or no binding of APSema3F to corresponding sections of brains from *Npn-2*$^{-/-}$ mice was detected (Figure 2B). A very low amount of APSema3F bound hippocampal projections and the corpus callosum of *Npn-2*$^{-/-}$ mice (Figure 2B; data not shown), which is likely the result of binding of APSema3F to Npn-1. *Npn-1* is expressed in the hippocampus and in cortical neurons that give rise

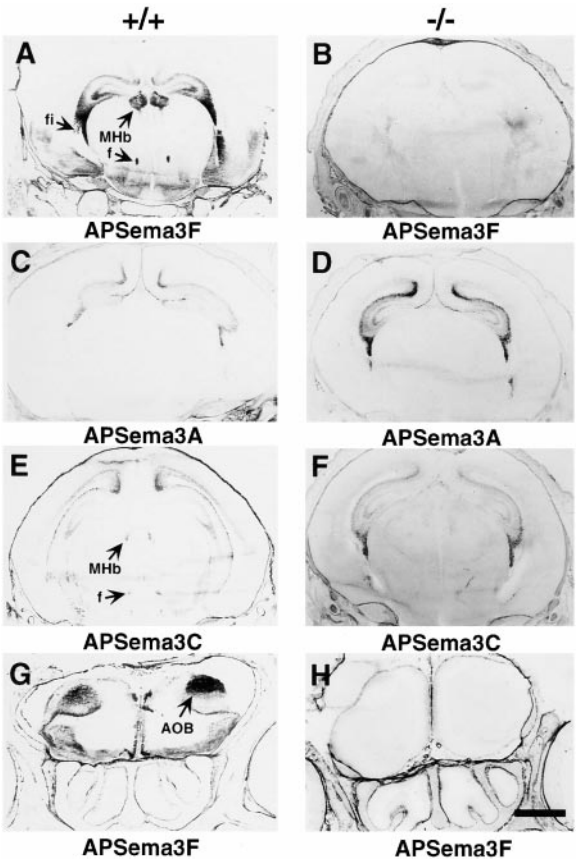

Figure 2. Binding of Class 3 Semaphorins to Endogenous Receptors in Wild-Type and *neuropilin-2* Homozygous Mutant Neonatal Brains

Coronal sections of either wild-type (A, C, E, and G) or *Npn-2* homozygous mutant (B, D, F, and H) P1 mouse brains were incubated with either APSema3F (A, B, G, and H), APSema3A (C and D), or APSema3C (E and F). See text for details. MHb, medial habenula; f, fornix; fi, fimbria; AOB, accessory olfactory bulb. Scale bar is 1.2 mm in (A) through (F), and 600 μm in (G) and (H). For APSema3F, APSema3A, and APSema3C; n = 7 (+/+), 7 (+/−), and 7 (−/−).

to the corpus callosum (Kawakami et al., 1996; Polleux et al., 1998), and Sema3F can bind to Npn-1, although with much lower affinity than to Npn-2 (Chen et al., 1997). Robust APSema3F binding was also detected in the accessory olfactory bulb and medial habenula in wild-type mice, but these structures were devoid of APSema3F binding activity in *Npn-2*$^{-/-}$ mice (Figures 2A, 2B, 2G, and 2H). The accessory olfactory bulb and medial habenula normally expresses *Npn-2* but not *Npn-1* (Kawakami et al., 1996; Chen et al., 1997; Giger et al., 1998). These results indicate that Npn-2 is the major binding site for Sema3F in the brain. In contrast, binding sites for APSema3A, an Npn-I ligand, appeared to be intact in neonatal brains of *Npn-2*$^{-/-}$ mice. For example, binding of APSema3A to the corpus callosum and the hippocampal formation of wild-type, heterozygous, and *Npn-2*$^{-/-}$ mice is very similar (Figures 2C and 2D; data not shown). Lastly, binding of APSema3C, which can bind to either Npn-1 or Npn-2 (Chen et al., 1997; Feiner et al., 1997; Takahashi et al., 1998), was partially diminished in brains of *Npn-2*$^{-/-}$ mice. APSema3C bound to

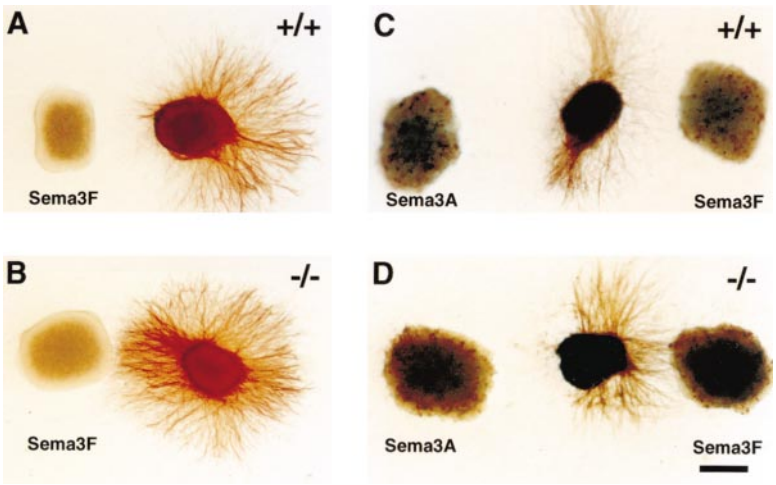

Figure 3. Sympathetic Neurons from *neuropilin-2* Homozygous Mice Are Unresponsive to Sema3F

SCG explants from either wild-type (A and C) or *Npn-2* homozygous mutant (B and D) E15 (A and B) or P1 (C and D) mice were cocultured in a collagen matrix with aggregates of COS cells expressing either Sema3F (A and B) or a combination of two COS cell aggregates expressing Sema3A and Sema3F (C and D). After 4 days of growth in vitro, the explants were fixed and stained with either antibodies against tyrosine hydroxylase, a marker for sympathetic neurons (A and B), or neurofilament-M (NF-M) (C and D). Sympathetic neurons from all wild-type and all *Npn-2* heterozygous mice are repelled by Sema3F and Sema3A, whereas neurons from all *Npn-2* homozygous mutant mice are repelled by Sema3A but not by Sema3F (see the Experimental Procedures for scoring criteria). For explants from E15 embryos: n = 4 (+/+), 9 (+/−), and 5 (−/−). For explants from P1 neonates cultured with Sema3F aggregates: n = 5 (+/+), 27 (+/−), and 6 (−/−); cultured with Sema3A aggregates: n = 3 (+/+), 5 (+/−), and 4 (−/−); cultured with both Sema3F and Sema3A aggregates: n = 2 (+/+), 3 (+/−), and 2 (−/−). Scale bar is 400 μm.

regions of the brain in which either one or both neuropilins are expressed, including the hippocampus and medial habenula (Figure 2F) and the corpus callosum (data not shown). APSema3C binding to the hippocampus, which normally expresses both neuropilins, is detected in *Npn-2*$^{-/-}$ mice (Figure 3F). The strongly reduced but still detectable binding of APSema3C to the fornix in *Npn-2*$^{-/-}$ mutants is likely to reflect a loss of binding to *Npn-2*-expressing septal afferents, while binding to CA3 efferents that normally express both neuropilins remains intact. APSema3C binding to the medial habenula, which normally expresses Npn-2, but not Npn-1, is not observed in *Npn-2*$^{-/-}$ mice (Figure 2F) even though this brain structure is present (data not shown). Thus, Npn-2 is the major binding site for Sema3F and one of the binding sites for Sema3C, but not Sema3A, in neonatal mouse brain.

Sympathetic Neurons from *Npn-2*$^{-/-}$ Mice Are Unresponsive to Sema3F In Vitro

We have previously shown that Sema3F secreted from COS cell aggregates repels axons of sympathetic neurons of the superior cervical ganglion (SCG) in vitro. This repulsion was attenuated when antibodies directed against Npn-2 were included in the culture medium, indicating that Npn-2 is essential for Sema3F signaling (Giger et al., 1998). To assess whether neurons from *Npn-2*$^{-/-}$ mice are deficient in Sema3F signaling, we performed in vitro repulsion assays in collagen matrices with SCGs dissected from either E15 embryos or P1 pups. Neurons were immunostained with antibodies directed against tyrosine hydroxylase (TH), a marker for sympathetic neurons. Sympathetic neurons from E15 and P1 wild-type or *Npn-2* heterozygous mice are strongly repelled by Sema3F secreted from COS cell aggregates (Figure 3A; data not shown). In contrast, fibers emanating from SCG explants obtained from *Npn-2*$^{-/-}$ mice are not repelled by Sema3F (Figure 3B). SCGs from wild-type, heterozygous, and *Npn-2*$^{-/-}$ mice were tested in coculture paradigms in which the ganglion is grown near COS cell aggregates secreting Sema3A alone (data not shown) or flanked on either side by COS cells secreting either Sema3F or Sema3A (Figures 3C and 3D). Wild-type and *Npn-2*$^{+/-}$ SCGs are repelled by both Sema3F and Sema3A. In contrast, *Npn-2*$^{-/-}$ sympathetic neurons are repelled by Sema3A but not by Sema3F. These results show that Npn-2 is an essential component of the receptor for Sema3F but not Sema3A.

Cranial Nerves Are Defective in *Npn-2*$^{-/-}$ Mice

Whole-mount in situ hybridization of E11 rat embryos revealed robust and widespread expression of *Npn-2* in the developing rodent nervous system as well as in several nonneural structures (Figure 5A). Prominent staining was seen in the basal forebrain, presumptive cranial nerve nuclei in the mid- and hindbrain anlagen, the developing sympathetic chain, and segmentally along the anterior–posterior axis in what appears to be early dorsal root ganglia. Nonneuronal *Npn-2* expression was most intense in the abdominal region in close proximity to the developing intestine, portions of the maxillary and mandibular processes, and fore- and hindlimb buds.

To test whether Npn-2 is required for axon pathfinding in vivo, we performed antineurofilament (2H3) immunohistochemistry (Dodd et al., 1988) on whole-mount preparations to visualize projections of cranial and spinal nerves in wild-type, *Npn-2*$^{+/-}$, and *Npn-2*$^{-/-}$ embyros. In E11 wild-type embryos, the major branches of cranial and spinal nerves are clearly stained with the 2H3 monoclonal antibody (Figure 4A). In marked contrast, trajectories of several cranial nerves in *Npn-2*$^{-/-}$ embryos were either disorganized or absent.

The oculomotor nerve in wild-type embryos normally projects as a tight fiber bundle from the mesencephalic flexure ventrally toward the cilliary ganglion and extrinsic ocular muscles. In *Npn-2*$^{-/-}$ embryos, this nerve is severely defasciculated; however, it still projects to its normal target field (Figures 4A–4D). Strikingly, the trochlear nerve, which normally exits the central nervous system at the dorsal hindbrain–midbrain junction and then projects to the superior oblique muscle of the eye, is

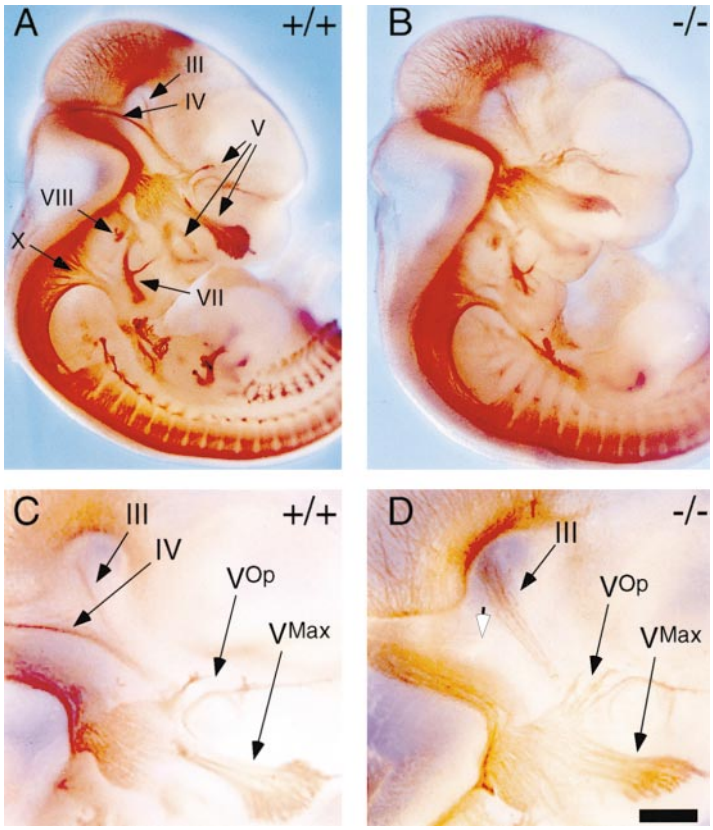

Figure 4. Cranial Nerves Are Defective in *neuropilin-2* Homozygous Mutant Mice

Whole-mount immunostaining using neurofilament antibodies (2H3) of wild-type (A and C) and *Npn-2* homozygous mutant embryos (B and D) at E11. The trochlear nerve is absent (open arrow in [D]), and the oculomotor nerve, branches of the trigeminal nerve, and the facial nerve are partially defasciculated in all *Npn-2* homozygous mutant embryos but not in any $Npn\text{-}2^{+/+}$ or $Npn\text{-}2^{+/-}$ embryos. III, oculomotor nerve; IV, trochlear nerve; V, trigeminal nerve; Vop, opthalmic branch of the trigeminal nerve; Vmax, maxillary branch of the trigeminal nerve; VII, facial nerve; VIII, vestibulocochlear nerve; and X, vagus nerve. Scale bar is 500 μm in (A) and (B), and 250 μm in (C) and (D). n = 13 (+/+), 16 (+/−), and 11 (−/−).

absent in $Npn\text{-}2^{-/-}$ embryos (Figures 4A–4D). Staining using antibodies against acetylcholinesterase showed the presence of the trochlear nucleus in E18 $Npn\text{-}2^{-/-}$ mice (data not shown). Moreover, antineurofilament immunohistochemistry revealed the presence of disorganized trochlear neuron projections within the CNS of E13.5 $Npn\text{-}2^{-/-}$ mice (data not shown). These results indicate that the trochlear nerve defect in $Npn\text{-}2^{-/-}$ mice is likely due to aberrant pathfinding and not a requirement for Npn-2 for differentiation, migration, or survival of trochlear motor neurons. Moreover, while the ophthalmic, maxillary, and mandibular branches of the trigeminal nerve of $Npn\text{-}2^{-/-}$ mice reach their target fields, regions of these nerves are uncharacteristically defasciculated in the proximal portion of their trajectory (Figures 4C and 4D). The $Npn\text{-}2^{-/-}$ ophthalmic branch of the trigeminal nerve has more terminal branches than are seen in wild-type embryos. In addition, the facial nerve in $Npn\text{-}2^{-/-}$ embryos projects toward its target field within the second branchial arch where it exhibits a characteristic bifurcation; however, the distal regions of both branches of this nerve defasciculate into abnormal small bundles in $Npn\text{-}2^{-/-}$ embryos (Figures 4A and 4B). The morphology of other cranial nerves, including the vestibulocochlear and vagus nerves, appear normal in $Npn\text{-}2^{-/-}$ embryos as assessed by whole-mount 2H3 immunohistochemistry.

Trochlear Motor Axons Are Repelled by Sema3F In Vitro

To address whether trochlear motor axons are directly responsive to Sema3F, we performed repulsion assays in collagen matrices using hindbrain–midbrain junction (HMJ) explants obtained from E11 rat embryos that include the trochlear nucleus (Colamarino and Tessier-Lavigne, 1995). Trochlear motor axons were visualized with the F84.1 monoclonal antibody that specifically labels motor axons (Prince et al., 1992). Trochlear motor axons emanating from HMJ explants approached aggregates of control COS cells robustly and showed no evidence of being repelled (Figure 5E). In contrast, HMJ explants cultured together with COS cell aggregates secreting Sema3F showed dramatic evidence of repulsion (Figure 5F). These axons turn away from the Sema3F source, demonstrating that trochlear motor axons are repelled by Sema3F in vitro. We also performed HMJ repulsion assays with COS cells secreting Sema3A and Sema3C; in neither case did we observe trochlear motor axon repulsion by these class 3 semaphorins (data not shown).

Whole-mount in situ hybridization at E11 in the rat and mouse shows prominent *Sema3F* expression in the caudal midbrain and the rostral hindbrain with a striking gap, however, at the hindbrain–midbrain junction (Figure 5B; data not shown). This is precisely the axial level where the trochlear nerve exits the CNS and establishes its contralateral peripheral projection to the eye. *Sema3F* is also expressed in the dorsal telencephalic vesicle, around the dorsal surface of the eye anlage, in an increasing rostral to caudal gradient in the midbrain, in mesenchymal tissue marking the lateral and distal regions of the maxillary and mandibulary process, and in the second branchial arch. *Sema3F* expression laterally flanking the trochlear nerve trajectory is likely to provide

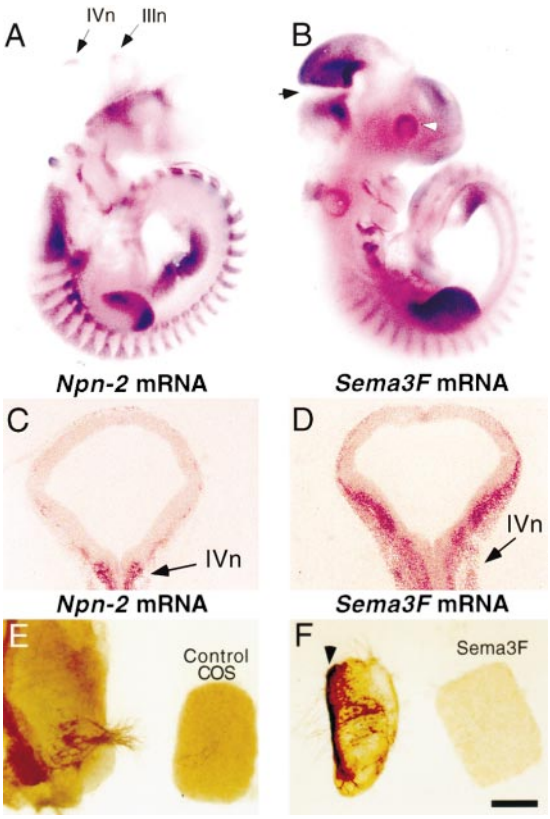

Figure 5. Sema3F, Npn-2, and the Establishment of the Trochlear Nerve Trajectory

(A and B) E11 whole-mount in situ hybridization for *Npn-2* (A) and *Sema3F* (B). *Sema3F* is expressed around the developing eye (open arrowhead) and in several other neuronal and nonneuronal structures (see text). Strikingly, *Sema3F* is not expressed at the hindbrain–midbrain junction, providing a channel through which the trochlear nerve extends into the periphery.

(C and D) Adjacent transverse sections through the hindbrain–midbrain junction region of E13 rat brains were processed for in situ hybridization using cRNA probes specific for *Npn-2* (C) and *Sema3F* (D). The trochlear nucleus is labeled by the *Npn-2* probe (arrow in [C]).

(E and F) Hindbrain–midbrain junction (HMJ) explants were cocultured with either control COS cell aggregates (E) or COS cell aggregates secreting Sema3F (F) and immunostained with F84.1 antibodies. In the presence of Sema3F, trochlear motor axons steer away from the Sema3F-secreting COS cell aggregates and extend in the opposite direction, often past the floor plate (arrowhead). n = 20 (APSema3F) and n = 25 (AP-Fc); all HMJ explants cultured adjacent to Sema3F, but not AP-Fc control, COS cell aggregates showed evidence of strong repulsion (see the Experimental Procedures for scoring criteria). Scale bar is 500 μm in (A) and (B), 250 μm in (C) and (D), and 375 μm in (E) and (F).

guidance information by creating inhibitory zones that direct trochlear motor axons and promote their fasciculation. To determine how Sema3F might function in directing trochlear motor axons within the CNS, we examined *Sema3F* expression in transverse sections at the level of the hindbrain–midbrain junction in E13 rat embryos. Adjacent transverse sections were hybridized with cRNA probes to reveal *Sema3F* transcript distribution and, in order to identify the trochlear nucleus, *Npn-2* expression. *Sema3F* is strongly expressed in the ventral lateral mantle zone at the hindbrain–midbrain junction.

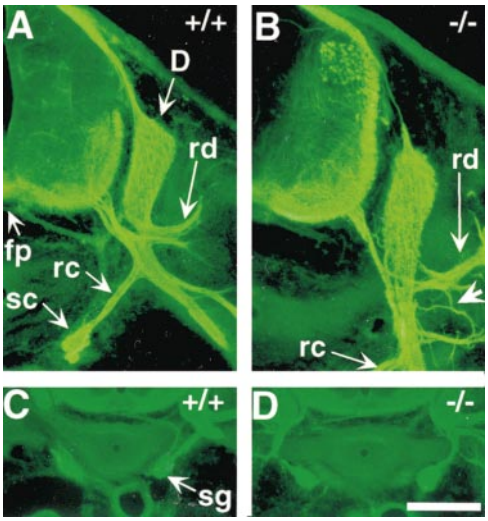

Figure 6. Spinal Neuron Projections Are Aberrant in *neuropilin-2* Homozygous Mutant Embryos

Transverse sections are shown from spinal cords of wild-type (A and C) and *Npn-2* homozygous mutant (B and D) mouse embryos at E12 (A and B) and E13.5 (C and D). Antibodies directed against neurofilament (2H3) were used to identify spinal nerves and the sympathetic chain ganglia. Branch points of spinal nerves are less compact and are partially defasciculated in all *Npn-2* mutant embryos but not in *Npn-2*$^{+/+}$ or *Npn-2*$^{+/-}$ embryos, resulting in aberrant extension of numerous individual fibers at several locations (for example, arrow in [B]). In both wild-type and *Npn-2* mutant embryos, the sympathetic ganglia appear normal (C and D). D, DRG; fp, floor plate; rd, dorsal ramus; rc, ramus communicantes; and sc, sympathetic chain. n = 6 (+/+), 4 (+/−), and 9 (−/−). Scale bar is 300 μm (A and B) and 600 μm (C and D).

This expression extends circumferentially with reduced and more lateral expression toward the dorsal CNS (Figures 5C and 5D). *Sema3F* mRNA is absent from the dorsal neural tube in the location where trochlear motor axons exit the CNS. These results show that trochlear motor neurons express *Npn-2*, are repelled by Sema3F in vitro, and that the spatial and temporal distribution of *Sema3F* mRNA in the CNS and periphery prefigures the central and peripheral trajectories of trochlear motor axons. This strongly suggests that a lack of Npn-2-mediated Sema3F repulsion produces the striking trochlear nerve phenotype observed in *Npn-2* mutant mice.

Spinal Nerve Branch Points Are Less Compact in *Npn-2*$^{-/-}$ Mice

Npn-2 normally is expressed in several neuronal populations that project axons into the periphery through spinal nerves including sensory DRG, motor, and sympathetic neurons (Chen et al., 1997; Kolodkin et al., 1997). Therefore, we examined sensory, motor, and sympathetic spinal nerve components using antineurofilament (2H3) and anti-TAG-1 (4D7) immunohistochemistry in *Npn-2* mutant mice. In contrast to wild-type and *Npn-2*$^{+/-}$ littermates, spinal nerves of *Npn-2* mutant embryos observed in transverse spinal cord sections of E12 (Figures 6A and 6B) and E14 (data not shown) appeared less compact and were defasciculated at major branch points. These branch points include the segregation of the dorsal ramus and ramus communicantes from the

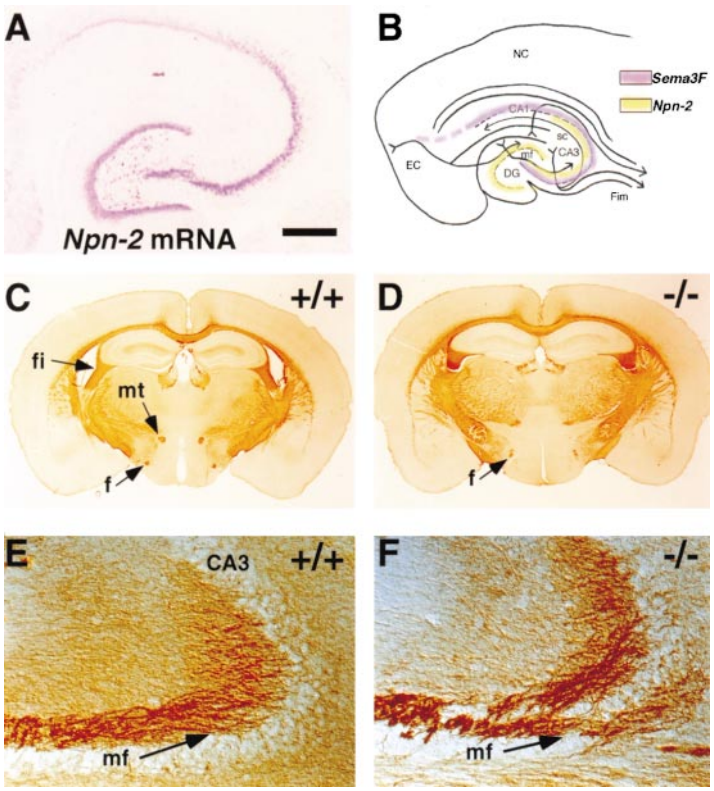

Figure 7. Extrinsic and Intrinsic Hippocampal Projections Are Defective in the Brains of *neuropilin-2* Homozygous Mutant Mice

Coronal sections through wild-type (C and E) and *Npn-2* mutant (D and F) adult brains are shown after immunohistochemistry with neurofilament antibodies (2H3) in order to illuminate hippocampal projections. For comparison, the distribution of *Npn-2* mRNA is shown in the adult brain (A), and a schematic of the adult hippocampal formation with *Npn-2*-expressing structures in green and *Sema3F*-expressing structures in purple is presented (B).

(A) *Npn-2* mRNA expression in the adult hippocampus is shown, demonstrating that neurons in the dentate gyrus that give rise to the mossy fibers express *Npn-2*, as do the CA3/CA1 pyramidal neurons and the hilus.

(B) A schematic of the adult hippocampus is shown illustrating intrahippocampal connectivity, major projections to and from the hippocampus, and the expression of mRNA for both *Npn-2* and *Sema3F*.

(C and D) In both wild-type and *Npn-2* mutant adult brains, the gross morphology of the hippocampal formation appears normal, including the fimbria (fi). However, in all *Npn-2* mutant brains, and in none of the *Npn-2*$^{+/+}$ or *Npn-2*$^{+/-}$ brains, the fornix (f) is reduced in size and appears fragmented into many small bundles (mt, mammillothalamic tract). n = 2 (+/+), 4 (+/−), and 5 (−/−).

(E and F) Higher magnification views of mossy fiber (mf) projections to the CA3 field reveal dramatic defects in *Npn-2* mutants. Rather than extending to, but not beyond, the CA3 pyramidal cell dendrites as in wild-type (C), mossy fibers in all *Npn-2* mutant brains, but not in *Npn-2*$^{+/+}$ or *Npn-2*$^{+/-}$ brains, grow deep into the distal stratum pyramidale of the CA3 field, occasionally entering into the stratum oriens.

Scale bar is 1.3 mm in (A), 130 μm in (C) and (D), and 325 μm in (E) and (F).

main spinal nerve (Figures 6A and 6B). The sensory fibers of spinal nerves visualized using anti-TAG-1 (Wolfer et al., 1994) showed similar defects (data not shown). In contrast, in *Npn-1* and *Sema3A* mutant mice (Kitsukawa et al., 1997; Taniguchi et al., 1997), more severe disruption of spinal nerves was observed. This phenotype includes defasciculation of main spinal nerve trunks, crossing of the dorsal midline of the embryo by spinal nerve fibers, abnormal sensory innervation of the skin, and abnormal limb innervation. We did not observe these defects in *Npn-2* mutants as assessed by 2H3 whole-mount immunohistochemistry at E10, 11, and 12.5, suggesting a more limited requirement for Npn-2 than Npn-1 in spinal nerve formation. Sympathetic neurons express both neuropilins and are repelled by Sema3A and Sema3F in vitro. In *Sema3A*$^{-/-}$ mice, the sympathetic chain is severely disorganized (Taniguchi et al., 1997). In *Npn-2*$^{-/-}$ mice, we did not observe gross defects in the overall morphology of the sympathetic chain ganglia (Figures 6C and 6D). Commissural axons in E11 spinal cord visualized by TAG-1 staining appear unaltered in *Npn-2*$^{-/-}$ mice compared to *Npn-2*$^{+/-}$ and *Npn-2*$^{+/+}$ mice. In contrast, in E12 embryos we observed a less pronounced bundling of the ipsilateral projections of commissural axons in *Npn-2*$^{-/-}$ mice compared to *Npn-2*$^{+/-}$ and wild-type littermates (data not shown). Our results demonstrate a requirement for Npn-2 in establishing normal spinal nerve projections and are consistent with the spatial and temporal expression of *Npn-2*, the in vitro repellent effects of class 3 semaphorin ligands that bind Npn-2 on neuronal populations that project in spinal nerves, and the embryonic distribution of *Sema3F* and *Sema3C*.

Selective Brain Defects in the Hippocampus, Anterior Commissure, and Thalamus in *Npn-2*$^{-/-}$ Mice

The viability of *Npn-2* mutant mice allowed us to investigate the requirement for Npn-2 in brain development in regions where neuropilins and class 3 semaphorins are expressed but where an in vivo requirement for these proteins has not yet been demonstrated.

Hippocampal Mossy Fibers Overshoot Their Targets in the CA3 Field

Both *Npn-1* and *Npn-2* are strongly expressed in the developing and mature hippocampal formation, as are several class 3 secreted semaphorins including Sema3A, Sema3F, and Sema3C (Kitsukawa et al., 1995; Chédotal et al., 1998). In vitro repulsion assays demonstrate that Sema3A and Sema3F are potent repellents for axons emanating from dentate gyrus (DG), CA3, and CA1 explants (Chédotal et al., 1998; Steup et al., 1999). In addition, *Npn-2* is expressed in the DG, CA3, and at reduced levels in CA1, whereas *Sema3F* is not expressed in the DG but is expressed in the CA3 and CA1 fields (Chédotal et al., 1998) (Figures 7A and 7B). We used 2H3 immunohistochemistry on brain sections of

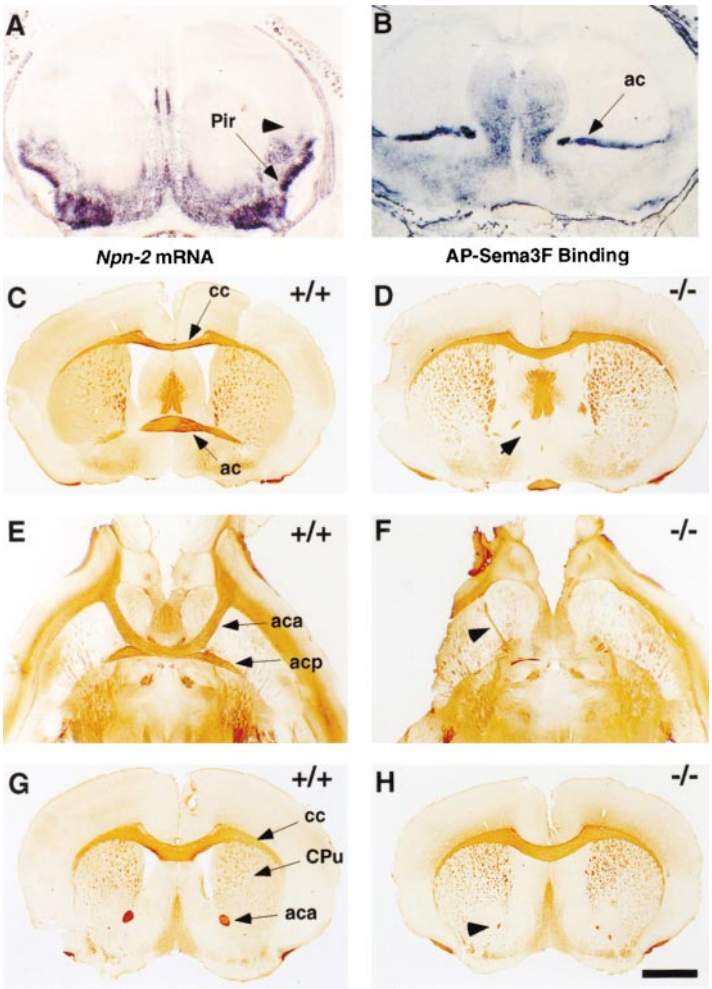

Figure 8. The Anterior Commissure Is Severely Disrupted in the Brains of *neuropilin-2* Homozygous Mutant Mice

Coronal sections of P1 rat brains at identical levels (A and B) are shown to reveal *Npn-2* mRNA expression (A) and endogenous Sema3F binding sites (B). Localization of *Npn-2* mRNA in a coronal section from a P1 brain shows that *Npn-2* is expressed at high levels in temporal, ventral cortex (including the piriform cortex [Pir]) and forms a sharp border with the dorsal neocortex (arrowhead). Binding of APSema3F to a coronal section from a P1 brain at the same level as in (A) shows localization of Sema3F binding sites on the anterior commissure (ac).

(C) through (H) Wild-type (C, E, and G) and *Npn-2* homozygous mutant (D, F, and H) adult brains are shown after immunohistochemistry with neurofilament antibodies (2H3) ([C], [D], [G], and [H], coronal sections; [E] and [F], horizontal sections). Coronal sections at the level where the anterior limb of the anterior commissure (aca) and the posterior limb of the anterior commissure (acp) cross the midline (C and D) reveal a complete loss of these crossing fibers in *Npn-2* mutant brains but normal ac morphology in all $Npn\text{-}2^{+/+}$ and $Npn\text{-}2^{+/-}$ brains. Horizontal sections show that the aca and acp are mostly absent in *Npn-2* mutants; however, remnants of these tracts are observed (arrowhead in [D]). Remnants of the aca can also be seen in coronal sections taken anterior to those in (C) and (D) so as to include only the aca component of the anterior commissure (arrowhead in [H]). The corpus callosum (cc) is normal in all *Npn-2* mutant brains (C, D, G, and H) (CPu, caudate putamen). $n = 3 (+/+)$, 6 $(+/-)$, and 7 $(-/-)$. Scale bar is 1.2 mm in (C) through (H), 600 μm in (A), and 450 μm in (B).

adult mice to investigate whether loss of Npn-2 results in hippocampal wiring defects. The most striking defects were observed in the mossy fiber projections of the dorsal hippocampus. In wild-type mice, the axons of dentate granule cells (mossy fibers) grow in the striatum lucidum along the inner surface of the CA3 principal cell layer and do not extend deep into the distal stratum pyramidale of CA3. In *Npn-2* mutant mice, mossy fibers follow their initial projection in the stratum lucidum. However, numerous fiber bundles grow too far laterally in the CA3 field, entering deep into the stratum pyramidale of CA3 and in some instances growing beyond into the stratum oriens (Figures 7E and 7F). These results are consistent with Sema3F in the CA3 acting as a repellent in vivo to facilitate correct targeting of DG mossy fibers to the CA3 field.

The fimbria and fornix carry both efferent fibers from the hippocampal formation and also subcortical (septal) afferent fibers to the hippocampal formation. Some axons of CA3 pyramidal cells also project in the hippocampal commissure, which joins the right and left hippocampi. CA3 neurons express both neuropilins, and septal neurons express *Npn-2* but not *Npn-1*.

In *Npn-2* mutants, the fornix is present but appears less tightly bundled when compared to wild-type mice (Figures 7C and 7D). Whether the malformation of the fornix seen in *Npn-2* mutant mice is the result of altered septal afferents and/or CA3 hippocampal efferents remains to be determined. The ventral hippocampal commissure, however, appears normal in all mutants examined, suggesting that contralateral hippocampal connectivity is generated in the absence of Npn-2-class 3 semaphorin guidance interactions.

Anterior Commissure Is Severely Abnormal

In addition to defects in hippocampal connectivity, we observed fully penetrant defects elsewhere in the limbic system where *Npn-2* is strongly expressed. In the basal forebrain of late embryos and in neonates, high levels of *Npn-2* expression are observed in ventral and temporal cortices including large regions of the rhinencephalon and cortical amygdala forming a sharp border at the dorsally located neocortex (Figure 8A) (Chen et al., 1997). Binding of APSema3F to endogenous receptors in corresponding forebrain sections is prominent on the anterior and posterior limbs of the anterior commissure (ac), a major interhemispheric connection linking temporal cortices and olfactory structures (Figure 8B). In coronal and horizontal sections of *Npn-2* mutant mice, we observe dramatic loss of both anterior and posterior limbs of the ac (Figures 8C–8H). A few thin fiber bundles are occasionally present in homozygous mutant brains and appear to be the remnants of the ac (Figure 8F). It is important to note that in *Npn-2* mutant neonatal and

adult brains we did not observe defects in other brain commissures, including the corpus callosum and the hippocampal commissure (Figures 8C, 8D, 8G, and 8H; data not shown).

Thalamic Projections from the Medial Habenula Are Defective

Npn-2 is expressed at high levels in the medial habenula of the thalamus starting as early as E12 and continuing into adulthood (Chen et al., 1997; Giger et al., 1998). *Sema3F* is expressed at similar high levels along the ventricular zone of the third ventricle, medially flanking the initial trajectory of the fasciculus retroflexus (habenulo-interpeduncular tract), which originates from thalamic neurons in the medial habenula and projects caudo-ventrally to innervate the interpeduncular nucleus (Giger et al., 1998). Endogenous Sema3F binding sites, visualized using in situ APSema3F ligand binding to E18 brain sections, are found on several tracts in the developing brain and spinal cord, and the fasciculus retroflexus is one of the most robust binding sites for this ligand at this developmental stage (Figure 9A). These data suggest that Sema3F and Npn-2 play important roles in establishing this thalamic tract. In support of this hypothesis, we observe a marked reduction in the size and organization of the fasciculus retroflexus in *Npn-2* mutant adult brains. Horizontal sections through adult brains were stained with monoclonal antibodies against MAP-2 allowing for observation of the fasciculus retroflexus in wild-type brains as a prominent tract adjacent to the parafascicular thalamic nucleus (Figure 9B). In similar sections from *Npn-2* mutant brains, however, the fasciculus retroflexus is much smaller in size and often appears to be represented by multiple smaller tracts in the region where normally a single large tract projects (Figure 9C). Morphology of the medial habenula, assessed with nissl stain, appears normal in *Npn-2* mutant brains, strongly suggesting that Npn-2 is not affecting the development of this nucleus. Taken together, these results show that CNS defects in *Npn-2* mutant brains are restricted to *Npn-2*-expressing pathways, demonstrating an in vivo role for Npn-2 in selectively translating guidance information from a subset of class 3 secreted semaphorins.

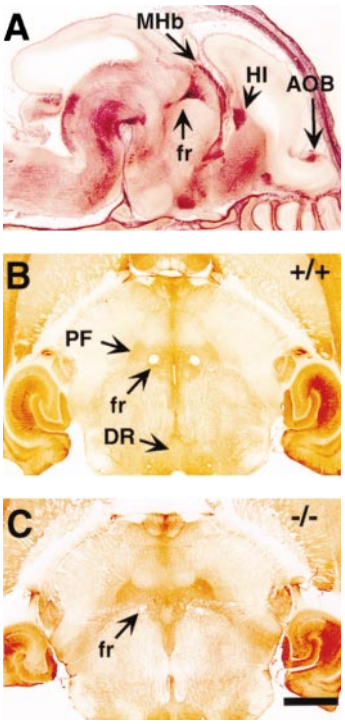

Figure 9. Thalamic Projections from the Medial Habenula Are Disorganized in *neuropilin-2* Homozygous Mutant Mice

(A) APSema3F binding to endogenous receptors is shown in a parasagital section of an E18 rat brain. High binding levels are observed in the medial habenula (MHb) of the thalamus and on the fasciculus retroflexus (fr), which projects caudo-ventrally from the MHb to the interpeduncular nucleus. APSema3F binding is also observed in several other locations, including the hippocampus (HI) and accessory olfactory bulb (AOB).

(B and C) Horizontal sections through adult wild-type (B) and *Npn-2* homozygous mutant (C) brains at the level of the dorsal raphe nucleus (DR) and parafascicular thalamic nucleus (PF) were stained with a MAP-2 monoclonal antibody to reveal the fasciculus retroflexus (fr). The fr at this level is a well-defined tract in all *Npn-2*$^{+/+}$ and *Npn-2*$^{+/-}$ brains, which appears as a circular absence of MAP-2 immunoreactivity. In all *Npn-2* mutants, the fr appears as several abnormally small tracts adjacent to the normal position of the fr. n = 1 (+/+), 2 (+/−), and 2 (−/−). HI, hippocampus. Scale bar is 1.2 mm.

Discussion

During development, different populations of neurons extend axons whose growth cones encounter a myriad of guidance cues, and among these are the secreted class 3 semaphorins. Though most of these structurally related semaphorins share the ability to function as repellents in vitro, they are each expressed in unique and dynamic patterns during development. Further, at least three of these class 3 semaphorins are functionally distinct, repelling different subsets of neuronal populations in vitro. Neuropilins bind selectively to subsets of class 3 semaphorins and also mediate the functional responses of different populations of neurons to these repellents. Therefore, in order to understand how class 3 semaphorins influence axon guidance decisions in vivo, we have generated mice with a null mutation at the *Npn-2* locus. Our results show that Npn-2 is required for the proper development of trajectories from a subset of CNS and PNS neuronal populations. The defects observed in *Npn-2* mutants, in combination with in vitro repulsion assays and the distribution of class 3 semaphorin transcripts and endogenous binding sites throughout neural development, suggest that loss of Npn-2 function results in an inability of several distinct populations of neurons to respond to Sema3F. Taken together with known functions of neuropilins and class 3 semaphorins, our results show that neuropilins, acting as class 3 semaphorin receptors, play an integral role in imparting selective responses to secreted semaphorins in vivo.

Npn-2 Is the Major Receptor for Sema3F and Is Required for Sema3F-Mediated Chemorepulsion In Vivo

Our work provides evidence that Npn-2 is the major receptor for Sema3F in the nervous system. The AP-Sema3F ligand binds to numerous projections in the CNS and PNS that normally express *Npn-2*, and brain

sections of *Npn-2* homozygous mutant mice exhibit very little APSema3F binding activity. Moreover, sympathetic neurons isolated from *Npn-2* mutant mice are completely unresponsive to Sema3F in vitro, while they remain responsive to Sema3A. These results strongly support the idea that Npn-1 and Npn-2 are Sema3A and Sema3F receptors, respectively. Whether Npn-2 is also required for Sema3C signaling in vivo, however, remains unclear. APSema3C binding to brains of wild-type and Npn-2 homozygous mutant mice shows that Sema3C, unlike Sema3A and Sema3F, can bind to brain structures expressing Npn-1 and/or Npn-2. This is commensurate with the observation that Sema3C binds with equal affinity to both Npn-1- and Npn-2-expressing COS cells. (Chen et al., 1997). In light of recent findings that distinct neuropilin and plexin family members are components of class 3 semaphorin holoreceptors (Takahashi et al., 1999; Tamagnone et al., 1999), it will be of interest to determine the exact molecular composition of the receptor complexes that mediate Sema3A, Sema3C, and Sema3F repulsive axon guidance events. While Npn-1 and Npn-2 are obligate coreceptors for Sema3A and Sema3F, respectively, a model for Sema3C function has been proposed in which both neuropilins are required (Chen et al., 1998; Takahashi et al., 1998). For example, sympathetic neurons express Npn-1 and Npn-2 are repelled by Sema3C, and antibody perturbation experiments have shown that Npn-1 is a necessary component of the Sema3C receptor (Chen et al., 1997; Feiner et al., 1997). Furthermore, sensory DRG neurons express Npn-1 but not Npn-2 and are not responsive to Sema3C. This model predicts that Sema3C signaling should be compromised in neurons from *Npn-2* mutant mice. Our efforts to establish whether Npn-2 is required for Sema3C signaling, however, have so far been unsuccessful. We have been unable to observe Sema3C repulsion of murine sympathetic neurons in vitro, despite multiple attempts using SCG explants from mice (both *Npn-2*$^{+/+}$ and *Npn-2*$^{-/-}$) isolated at several developmental stages ranging from E14 to P1. Yet, under our experimental conditions, equivalent amounts of Sema3A and Sema3F released from COS cell aggregates potently repel axons emanating from the SCG explants. Therefore, in our hands Sema3C is a poor repellant for murine sympathetic neurons in vitro, and whether Npn-2 is required for Sema3C signaling in vivo remains an open question.

Since *Npn-2* mutant mice exhibit defects in binding activity of both Sema3F, and to a lesser extent Sema 3C, the neural defects observed in *Npn-2* mutant mice may be due to a decrease in signaling by Sema3F, Sema3C, or other class 3 semaphorins. We favor a model in which many of the neural defects in *Npn-2* mutant mice result from a deficiency in Sema3F-Npn-2 signaling. This idea is supported by our observations that sympathetic neurons from *Npn-2* mutant mice are completely unresponsive to Sema3F in vitro and that spatial and temporal distribution of *Sema3F* mRNA in the CNS and periphery prefigures the trajectories of many projections we found to be defective in *Npn-2* mutants. An important test of this model will come from future studies that will compare the integrity of the nervous system in *Npn-2*, *Sema3F*, and *Sema3C* mutant mice.

Npn-2 Is Required for Normal Projections of Cranial and Spinal Nerves

A striking finding in the present study is that many *Npn-2* mutant mice survive into adulthood despite the existence of numerous neurological deficits. Also noteworthy is the observation that some of the neural defects observed in *Npn-2* mutant mice are complementary to those observed previously for *Npn-1* mutant mice. This point is well illustrated by comparing cranial nerve defects in the two *neuropilin* mutants. In mice lacking *Npn-1*, many cranial nerves are disorganized and/or defasciculated, including all branches of the trigeminal nerve, the facial nerve, the glossopharyngeal nerve, and the vagus nerve (Kitsukawa et al., 1997). Importantly, in *Npn-1* mutant animals the oculomotor and trochlear nerves appear normal. In dramatic contrast, *Npn-2* mutants show severe defasciculation of the oculomotor nerve and absence of the peripheral projection of the trochlear nerve (Figure 4). Interestingly, in vitro coculture experiments showed that oculomotor motor axons are not repelled by Sema3A, though in this same study trochlear motor axons were observed to be repelled by Sema3A (Varela-Echavarria et al., 1997). We did not observe Sema3A or Sema3C repulsion of trochlear neurons (data not shown), while we did observe a clear repulsive response by these neurons to Sema3F. Though the oculomotor nucleus and trochlear nucleus do not initially express *Npn-1* at high levels (cited in Kitsukawa et al., 1997), in the present study we observe *Npn-2* expression in these cranial nuclei at E13 in the rat. The dramatic trochlear nerve phenotype in *Npn-2* mutant embryos, coupled with embryonic *Sema3F* expression in the CNS and in the periphery, suggest an important role for Sema3F and Npn-2 in establishing this trajectory. Sema3F in the CNS is likely to provide a strong repulsive cue for trochlear neurons in their initial dorsal trajectory. Together with previous work showing that netrin-1 can repel trochlear neurons in vitro (Colamarino and Tessier-Lavigne, 1995), this suggests that semaphorins and netrins work in concert to guide trochlear motor neurons within the CNS. Following their dorsal decussation and exit from the CNS at the hindbrain–midbrain junction, peripheral Sema3F is likely to channel trochlear motor neurons, promoting their fasciculation and defining their peripheral trajectory. Interestingly, we have observed a dramatic misalignment of the pupils in eyes of some *Npn-2* mutant adult mice (unpublished data), suggesting that defects in eye muscle innervation resulting from aberrant Sema3F-Npn-2 signaling may underlie certain types of strabismus.

Differences between the *Npn-1* and *Npn-2* mutant mice are also observed in projections of other peripheral nerves. In both *Npn-1* and *Npn-2* mutant mice, some spinal nerve fibers prematurely exit the nerve trunks. However, in *Npn-1* mutants but not *Npn-2* mutants distal projections of spinal nerves are highly disorganized, and some fibers cross the dorsal midline and project abnormally to the skin and limbs (Kitsukawa et al., 1997). Similarly, the vagus nerve is defective in *Npn-1* mutant mice but appears normal in *Npn-2* mutants. Some cranial nerves, including the ophthalmic and maxillary branches of the trigeminal and the facial nerve, are defective in both *Npn-1* and *Npn-2* mutant mice. Taken

together, *Npn-1* mutants and *Npn-2* mutants have overlapping but distinct defects in peripheral nerves. This suggests that in many neuronal populations in vivo neuropilins function independently of each other to selectively respond to different class 3 semaphorins.

Npn-2 Is Required for the Development of Several Limbic Tracts

Since a significant fraction of *Npn-2* mutant mice survive into adulthood, we were able to assess the role played by *Npn-2* in the establishment of major CNS pathways. We observed several discrete defects that are restricted to those tracts that, based on *Npn-2* expression and/or the presence of APSema3F binding sites, are likely to require Npn-2Sema3F signaling for their establishment.

Of particular interest are defects in hippocampal connectivity that include overshooting by DG mossy fibers of their targets in the CA3 field. Previous studies suggest that neuropilin class 3 semaphorin signaling is likely to play an important role in the stereotypic generation of correct hippocampal afferent and efferent trajectories (Chédotal et al., 1998; Steup et al., 1999). In particular, the expression of *Npn-2* in DG granule cells and *Sema3F* in CA3 and CA1 fields but not in the DG, and the repulsive effects of Sema3F on axons emanating from DG explants in vitro, suggest that the correct termination of DG mossy fibers on neurons in the CA3 field results from Sema3F-mediated repulsion (Chédotal et al., 1998). The mossy fiber projection defects we observe are consistent with this hypothesis. Though in vitro intrahippocampal repulsion between axons emanating from DG, CA1, and CA3 explants and these same hippocampal regions was not observed (Chédotal et al., 1998), this may simply reflect local sequestration of Sema3F on the DG mossy fiber target region in the CA3 and therefore a requirement for local interactions in guiding these axons. A similar situation, which awaits future analysis, may also occur in the generation of Schaffer collateral projections between the CA3 and CA1 fields. In addition to mossy fiber projection defects, we also observed defects in the fornix, which contains hippocampal afferent and efferent projections. Future analyses will provide a more detailed picture of the role played by Npn-2 in the establishment of hippocampal connectivity and, perhaps, the maintenance and remodeling of these connections during adult life. In this light, it is interesting to note that we have observed seizures in several *Npn-2* mutant mice (unpublished data).

In addition to hippocampal connectivity defects, we also observe dramatic and selective defects in other major limbic tracts in *Npn-2* mutant mice. These include an almost complete absence of both limbs of the anterior commissure and a severe disruption of the fasciculus retroflexus. These tracts share features that strongly suggest that these defects result from a loss of specific Sema3F-Npn-2 signaling events, including expression of *Npn-2* in the neuronal populations that contribute axons to these tracts and the presence of APSema3F binding sites (Chen et al., 1997; Giger et al., 1998; this study). In addition, expression of *Sema3F* supports a repulsive role for this class 3 semaphorin in the establishment of the fasciculus retroflexus during development (Giger et al., 1998). Interestingly, defects in the ac have also been reported in *netrin-1* and *EphB2* mutant mice (Henkemeyer et al., 1996; Serafini et al., 1996), showing that several distinct guidance molecules cooperate for the proper development of the ac.

The selectivity of the projection defects we observed in this study for *Npn-2*-expressing CNS and PNS neuronal populations throughout neural development supports the notion that neuropilins confer on neurons exquisite specificity with respect to guidance responses to class 3 semaphorins. Future analyses of the roles played by Npn-2 in target innervation by sympathetic neurons, the generation of connectivity in the olfactory system, and the generation of thalamo-cortical connectivity will provide additional tests of this hypothesis.

Experimental Procedures

Generation of *Npn-2*$^{-/-}$ Mice

Genomic DNA flanking the translation initiation site of the *Npn-2* gene was obtained from a mouse 129SVJ lambda FixII library (Stratagene) screened with a 388 bp EcoRI cDNA probe covering 5′-noncoding sequences and the first 33 amino acids of rat Npn-2. Two overlapping lambda clones λ4.1B (~15 kb) and λ17.1 (~18 kb) containing the first exon, presumptive promoter region, and part of intron 1 were isolated, restriction mapped, and partially sequenced. A 12.5 kb XbaI fragment containing exon 1, ~7.5 kb upstream sequences, and 4.5 kb of intron 1 was subcloned in pBlueScript and served as template for the construction of the targeting vector. The two arms of homology, a 6 kb SpeI fragment located approximately 1.7 kb upstream of exon 1, and a 2.6 kb PCR generated fragment located at the 5′-border of intron 1, were placed into the targeting backbone vector pTK-Neo3A (Rosahl et al., 1995). ES clones resistant to both G418 and gancyclovir (Thomas and Capecchi, 1987; Friedrich and Soriano, 1991) were expanded and analyzed by Southern blotting for the presence of a 3 kb BamHI fragment that is diagnostic of a homologous recombination event (see Figure 1A for targeting strategy and position of outside probe). Two correctly targeted ES cell clones were identified, and one was injected into C57BL/6-J-derived blastocysts. The resulting chimera from one of these, clone 1–225, produced germline offspring. For Southern blot analysis, 20 μg of tail genomic DNA was digested with BamHI and hybridized overnight at 60°C with a ^{32}P-dCTP radiolabeled 246 bp PCR fragment (Figure 1A). For rapid genotyping of mice, PCR reactions were performed using two pairs of oligonucleotides designed to amplify the wild-type (antisense, 5′AGAAGCCCGCTGAGATCT; and sense, 5′′CTCTCTGTCAAAAATGGATATG3′) and mutant alleles (sense, 5′CAGCTGTGCTCGACGTTGTC; and antisense, 5′ACGC TATGTCCTGATAGCGG). Northern analysis was performed with a ^{32}P-dCTP labeled 2558 bp rat cDNA EcoR1 fragment of the Npn-2 ectodomain, beginning 102 bp downstream of the first translation initiation codon, with total RNA from E15 wild-type, *Npn-2*$^{+/-}$, and *Npn-2*$^{-/-}$ embryos (Sambrook et al., 1989). Western blotting was performed on whole brain lysates from P1 mice (Giger et al., 1998).

Collagen Repulsion Assays

SCGs were dissected from E15 mouse embryos or P1 mice, and in vitro repulsion assays were done as previously described for rat SCGs (P1, Giger et al., 1998; E15, Chen et al., 1998). Trochlear motor neurons were dissected out from the hindbrain–midbrain junction (HMJ) of E11 rat embryos (obtained from timed-pregnant Sprague-Dawley rats) essentially as described (Colamarino and Tessier-Lavigne, 1995). Following dissection, ventral HMJ explants were cocultured for 40 hr with COS/293T cell aggregates secreting APSema3A, APSema3F, APSema3C, or APFc in collagen in culture medium (70:25 mix of OPTI-MEM and F12 medium [GIBCO] supplemented with Glutamax [GIBCO], 1% P/S, 40 mM glucose, and 5% calf serum). The criteria for lack of repulsion of SGC axons were radial and symmetrical fiber outgrowth from the SCG explant and a proximal to distal ratio of > 0.95. Repulsion was defined as asymmetrical fiber growth with a proximal to distal ratio of < 0.3.

Quantitation of neurite extension in trochlear repulsion assays

was determined by dividing the distance between HMJ explants and ligand-secreting COS cell aggregates (which was always between 300–500 μm) into two zones with a line between the two (similar to the method employed by Augsburger et al. [1999]). This was done such that extension of axons from the HMJ explants could be scored with respect to whether or not they passed a point one-third of the distance to the COS cell aggregates. For both control (APFc) and ligand (APSema3F) secreting aggregates, the approximate fraction of F84.1 positive axons from the ventral HMJ explant that crossed this line was determined. Repulsion was defined as >90% of fibers from the ventral HMJ not crossing the line; this was the case for all HMJ explants cocultured with AFSema3F-secreting COS cells. In contrast, in APFc HMJ cocultures, 100% of projections crossed this line.

In Situ Hybridization and AP-Fusion Protein Binding to Tissue Sections

The rat *Sema3F* template for riboprobe synthesis (nucleotides 697–2995) spans most of the ORF as previously described (Giger et al., 1998), and the rat *Npn-2* template is a 2558 bp EcoRI fragment of the Npn-2 ectodomain beginning 102 bp downstream of the first translation initiation codon (Kolodkin et al., 1997). For whole-mount in situ hybridization we followed a modified protocol from (Wilkinson and Nieto, 1993). AP-fusion protein binding to tissue sections was performed as described (Feiner et al., 1997).

Immunohistochemical Procedures

Mice were anesthetized and perfused transcardially with 120 ml of ice-cold perfusion solution [PBS containing 4% paraformaldehyde (PFA)]. Brains were dissected, post-fixed for 5 hr in perfusion solution, and cryoprotected overnight in PBS containing 10% dimethylsulfoxide. Forty micron sections of frozen brain were obtained using a freezing microtome and subsequently processed as free-floating sections. Endogenous peroxidase activity was quenched by incubation of sections in TBS (50 mM TrisHCL [pH 7.6] and 150 mM NaCl) containing 1% H_2O_2 and 10% methanol for 30 min, followed by several washes in TNT (50 mM TrisHCl [pH 7.6], 500 mM NaCl, and 0.5% Triton X-100). Then, sections were blocked for 2 hr in TNT containing 10% fetal bovine serum. Timed-pregnant females (plug day is E0) were sacrificed to obtain E10.5–E18 embryos. Embryos were sectioned (50–80 μm) and processed free-floating for immunofluorescence. Sections were washed in TNT and blocked in TNT containing 10% FBS for 2 hr. Primary antibodies for fixed embryonic and adult sections included antineurofilament 2H3 and anti-TAG-1 4D7 (supernatant from hybridoma cells, Developmental Hybridoma Bank), and anti-MAP-2 (Roche Molecular Biochemicals). Antibody incubations were performed overnight at 4°C in TNT containing 2% FBS. Sections were washed in TNT and incubated with the secondary antibodies for 1 hr at room temperature. Secondary antibodies included sheep anti-mouse Ig-HRP (Amersham), Cy3-donkey anti-mouse IgM, and FITC-donkey anti-mouse IgG (Jackson ImmunoResearch). Peroxidase stained brain sections were dehydrated in a graded series of ethanol solutions, cleared in Xylene, and embedded in DPX (Fluka). Embryonic sections were mounted in Fluoromount-G (Southern Biotechnology Associates) and imaged using a Zeiss axioplan microscope. For whole-mount antineurofilament immunohistochemistry of E10.5, E11, and E12 embryos, antineurofilament 2H3 supernatant was used (1:50) as described (Kitsukawa et al., 1997). Collagen explant cultures of SCGs and HMJs were fixed with 4% PFA in PBS at room temperature followed by incubation in PHT with either antityrosine hydroxylase (Incstar), antineurofilament (2H3), or anti-DM-GRASP antibody (F84.1) overnight at 4°C. After several washes in PHT, cultures were incubated with Sheep anti-mouse Ig-HRP secondary antibody, extensively washed in PHT, and developed with 3,3′ diaminobenzidine (DAB) in PBS.

Acknowledgments

We thank W. Stallcup for generously providing the F84.1 antibodies, M. Tessier-Lavigne and S. Strittmatter for APSema3C expression plasmids, and Mark Molliver and members of the Ginty and Kolodkin laboratories for helpful discussions. *Npn-2* mutant mice are the property of SmithKline Beecham Pharmaceuticals, and requests for these mice should be directed to F. S. W. This work was supported by the National Institutes of Health/National Institutes of Mental Health-R01MH59199 (D. D. G. and A. L. K.), the National Alliance for Research on Schizophrenia and Depression and Schweizerischen Nationalfonds (R. J. G.), the Medical Research Council of Canada (J.-F. C.), and a grant from SmithKline Beecham Neuroscience (R. G., D. D. G., and A. L. K.).

Received November 4, 1999; revised November 23, 1999.

References

Augsburger, A., Schuchardt, A., Hoskins, S., Dodd, J., and Butler, S. (1999). BMPs as mediators of roof plate repulsion of commissural neurons. Neuron *24*, 127–141.

Chédotal, A., Del Rio, J.A., Ruiz, M., He, Z., Borrell, V., de Castro, F., Ezan, F., Goodman, C.S., Tessier-Lavigne, M., Sotelo, C., et al. (1998). Semaphorins III and IV repel hippocampal axons via two distinct receptors. Development *125*, 4313–4323.

Chen, H., Chédotal, A., He, Z., Goodman, C.S., and Tessier-Lavigne, M. (1997). Neuropilin-2, a novel member of the neuropilin family, is a high affinity receptor for the semaphorins Sema E and Sema IV but not Sema III. Neuron *19*, 547–559.

Chen, H., He, Z., Bagri, A., and Tessier-Lavigne, M. (1998). Semaphorin-neuropilin interactions underlying sympathetic axon responses to class III semaphorins. Neuron *21*, 1283–1290.

Cheng, H.-J., and Flanagan, J.G. (1994). Identification and cloning of ELF-1, a developmentally expressed ligand for the Mek4 and Sek receptor tyrosine kinases. Cell *79*, 157–168.

Colamarino, S.A., and Tessier-Lavigne, M. (1995). Netrin-1 is a bifunctional axon guidance cue: long range repulsion of trochlear motor axons. Cell *81*, 621–629.

Comeau, M.R., Johnson, R., DuBose, R.F., Petersen, M., Gearing, P., VandenBos, T., Park, L., Farrah, T., Buller, R.M., Cohen, J.I., et al. (1998). A poxvirus-encoded semaphorin induces cytokine production from monocytes and binds to a novel cellular semaphorin receptor, VESPR. Immunity *8*, 473–482.

Dodd, J., Morton, S.B., Karagogeos, D., Yamamoto, M., and Jessell, T.M. (1988). Spatial regulation of axonal glycoprotein expression on subsets of embryonic spinal neurons. Neuron *1*, 105–116.

Feiner, L., Koppel, A.M., Kobayashi, H., and Raper, J.A. (1997). Secreted chick semaphorins bind recombinant neuropilin with similar affinities but bind different subsets of neurons in situ. Neuron *19*, 539–545.

Friedrich, G., and Soriano, P. (1991). Promoter traps in embryonic stem cells: a genetic screen to identify and mutate developmental genes in mice. Genes Dev. *5*, 1513–1523.

Giger, R.J., Urquhart, E.R., Gillespie, S.K.H., Levengood, D.V., Ginty, D.D., and Kolodkin, A.L. (1998). Neuropilin-2 is a receptor for semaphorin IV: insight into the structural basis of receptor function and specificity. Neuron *21*, 1079–1092.

Goodman, C.S., Kolodkin, A.L., Luo, Y., Püschel, A.W., and Raper, J.A. (1999). Unified nomenclature for the semaphorins/collapsins. Cell *97*, 551–552.

He, S., and Tessier-Lavigne, M. (1997). Molecular basis of axonal chemorepulsion: neuropilin is a semaphorin/collapsin receptor. Cell *90*, 739–751.

Henkemeyer, M., Orioli, D., Henderson, J.T., Saxton, T.M., Roder, J., Pawson, T., and Klein, R. (1996). Nuk controls pathfinding of commissural axons in the mammalian central nervous system. Cell *86*, 35–46.

Kawakami, A., Kitsukawa, T., Takagi, S., and Fujisawa, H. (1996). Developmentally regulated expression of a cell surface protein, neuropilin, in mouse nervous system. J. Neurobiol. *29*, 1–17.

Kawasaki, T., Kitsukawa, T., Bekku, Y., Matsuda, Y., Sanbo, M., Yagi, T., and Fujisawa, H. (1999). A requirement for neuropilin-1 in embryonic vessel formation. Development *126*, 4895–4902.

Kitsukawa, T., Shimono, A., Kawakami, A., Kondoh, H., and Fujisawa, H. (1995). Overexpression of a membrane protein, neuropilin, in chimeric mice causes anomalies in the cardiovascular system, nervous system and limbs. Development *121*, 4309–4318.

Kitsukawa, T., Shimizu, M., Sanbo, M., Hirata, T., Taniguchi, M., Bekku, Y., Yagi, T., and Fujisawa, H. (1997). Neuropilin-semaphorin III/D-mediated chemorepulsive signals play a crucial role in peripheral nerve projection in mice. Neuron *19*, 995–1005.

Kolodkin, A.L., Levengood, D.V., Rowe, E.G., Tai, U.-T., Giger, R.J., and Ginty, D.D. (1997). Neuropilin is a semaphorin III receptor. Cell *90*, 753–762.

Mark, M.D., Lohrum, M., and Püschel, A.W. (1997). Patterning neuronal connections by chemorepulsion: the semaphorins. Cell Tissue Res. *290*, 299–306.

Mueller, B.K. (1999). Growth cone guidance: first steps towards a deeper understanding. Annu. Rev. Neurosci. *22*, 351–388.

Ohta, K., Takagi, S., Asou, H., and Fujisawa, H. (1992). Involvement of neuronal cell surface molecule B2 in the formation of retinal plexiform layers. Neuron *9*, 151–161.

Ohta, K., Mizutani, A., Kawakami, A., Murakami, Y., Kasuya, Y., Takagi, S., Tanaka, H., and Fujisawa, H. (1995). Plexin: a novel neuronal cell surface molecule that mediates cell adhesion via a homophilic binding mechanism in the presence of calcium ions. Neuron *14*, 1189–1199.

Polleux, F., Giger, R.J., Ginty, D.D., Kolodkin, A.L., and Ghosh, A. (1998). Patterning of cortical efferent projections by semaphorin-neuropilin interactions. Science *282*, 1904–1906.

Prince, J.T., Nishiyama, A., Healy, P.A., Beasley, L., and Stallcup, W.B. (1992). Expression of the F84.1 glycoprotein in the spinal cord and cranial nerves of the developing rat. Dev. Brain Res. *68*, 193–201.

Rosahl, T.W., Spillane, D., Missler, M., Herz, J., Selig, D.K., Wolff, J.R., Hammer, R.E., Malenka, R.C., and Sudhof, T.C. (1995). Essential functions of synapsins I and II in synaptic vesicle regulation. Nature *375*, 488–493.

Sambrook, J., Fritsch, E.F., and Maniatis, T. (1989). Molecular Cloning: A Laboratory Manual, Second Edition (Cold Spring Harbor, NY: Cold Spring Harbor Laboratory Press).

Satoda, M., Takagi, S., Ohta, K., Hirata, T., and Fujisawa, H. (1995). Differential expression of two cell surface proteins, neuropilin and plexin, in *Xenopus* olfactory axon subclasses. J. Neurosci. *15*, 942–955.

Serafini, T., Colamarino, S.A., Leonardo, E.D., Wang, H., Beddington, R., Skarnes, W.D., and Tessier-Lavigne, M. (1996). Netrin-1 is required for commissural axon guidance in the developing vertebrate nervous system. Cell *87*, 1001–1014.

Soker, S., Takashima, S., Miao, H.-Q., Neufeld, G., and Klagsbrun, M. (1998). Neuropilin-1 is expressed by endothelial and tumor cells as an isoform-specific receptor for vascular endothelial growth factor. Cell *92*, 735–745.

Steup, A., Ninnemann, O., Savaskan, N.E., Nitsch, R., Püschel, A.W., and Skutella, T. (1999). Semaphorin D acts as a repulsive factor for entorhinal and hippocampal neurons. Eur. J. Neurosci. *11*, 729–734.

Takahashi, T., Nakamura, F., Jin, Z., Kalb, R., and Strittmatter, S. (1998). Semaphorins A and E act as antagonists of neuropilin-1 and agonists of neuropilin-2 receptors. Nat. Neurosci. *1*, 487–493.

Takahashi, T., Fournier, A., Nakamura, F., Wang, L.-H., Murakami, Y., Kalb, R.G., Fujisawa, H., and Strittmatter, S.M. (1999). Plexin-neuropilin-1 complexes form functional semaphorin-3A receptors. Cell *99*, 59–69.

Tamagnone, L., Artigiani, S., Chen, H., He, Z., Ming, G.-L., Song, H.-J., Chédotal, A., Winberg, M.L., Goodman, C.S., Poo, M.-M., et al. (1999). Plexins are a large family of receptors for transmembrane, secreted, and GPI-anchored semaphorins in vertebrates. Cell *99*, 71–80.

Taniguchi, M., Yuasa, S., Fujisawa, H., Naruse, I., Saga, S., Mishina, M., and Yagi, T. (1997). Disruption of semaphorin *III/D* gene causes severe abnormality in peripheral nerve projection. Neuron *19*, 519–530.

Thomas, K.R., and Capecchi, M.R. (1987). Site-directed mutagenesis by gene targeting in mouse embryo-derived stem cells. Cell *51*, 503–512.

Varela-Echavarria, A., Tucker, A., Püschel, A.W., and Guthrie, S. (1997). Motor axon subpopulations respond differentially to the chemorepellents netrin-1 and semaphorin D. Neuron *18*, 193–207.

Wilkinson, D.G., and Nieto, M.A. (1993). Detection of messenger RNA by in situ hybridization to tissue sections and whole mounts. Methods Enzymol. *225,* 361–373.

Winberg, M.L., Noordermeer, J.N., Tamagnone, L., Comoglio, P.M., Spriggs, M.K., Tessier-Lavigne, M., and Goodman, C.S. (1998). Plexin A is a neuronal semaphorin receptor that controls axon guidance. Cell *95*, 903–916.

Wolfer, D.P., Henehan-Beatty, A., Stoeckli, E.T., Sonderegger, P., and Lipp, H.P. (1994). Distribution of TAG-1/axonin-1 in fibre tracts and migratory streams of the developing mouse nervous system. J. Comp. Neurol. *345*, 1–32.